Crystal structure of the tRNA-specific adenosine deaminase from Streptococcus pyogenes

ARTICLE *in* PROTEINS STRUCTURE FUNCTION AND BIOINFORMATICS · SEPTEMBER 2007

Impact Factor: 2.63 · DOI: 10.1002/prot.21456 · Source: PubMed

9 AUTHORS, INCLUDING:

Eun Hye Lee
Korea University
28 PUBLICATIONS **154** CITATIONS
SEE PROFILE

Kwang Yeon Hwang
Korea University
125 PUBLICATIONS **2,525** CITATIONS
SEE PROFILE

WILEY InterScience® DISCOVER SOMETHING GREAT

PROTEINS STRUCTURE ■ FUNCTION ■ BIOINFORMATICS

STRUCTURE NOTE

Crystal structure of the tRNA-specific adenosine deaminase from *Streptococcus pyogenes*

Won-Ho Lee,[1] Young Kwan Kim,[1] Ki Hyun Nam,[1] Amit Priyadarshi,[1,2] Eun Hye Lee,[1] Eunice Eunkyeong Kim,[2] Young Ho Jeon,[3] Chaejoon Cheong,[3] and Kwang Yeon Hwang[1]*

[1] Division of Biotechnology, College of Life Sciences and Biotechnology, Korea University, Seoul 136-701, South Korea

[2] Biomedical Research Center, Korea Institute of Science and Technology, Seoul 136-791, South Korea

[3] Magnetic Resonance Team, Korea Basic Science Institute, Ochang, Chungbuk 363-883, Korea

Key words: adenosine deaminase; inosine; RNA editing; tRNA-specific; Streptococcus pyogenes.

INTRODUCTION

Nuclear pre-mRNA editing by selective adenosine deamination (A-to-I editing) occurs in all organisms from *C. elegans* to humans. The nucleotide inosine (I) has been observed in viral transcripts and in eukaryotic mRNAs. Inosine derives the deamination of adenosine (A), a process termed RNA editing. Inosine is not only present in mRNA, but also in tRNA, and was first identified in tRNA from yeast.[1] In the eukaryotes, seven to eight tRNAs contain I at position 34, whereas in prokaryotes and plant chloroplasts only the $tRNA^{Arg2}$ contains this modification. RNA editing of pre-mRNA is catalyzed by adenosine deaminase acting on RNA (ADARs). The ADARs are RNA editing enzymes that target double-stranded regions of nuclear-encoded RNA and viral RNA. These enzymes are particularly abundant in the nervous system, where they diversify information encoded in the genome, for example, by altering codons in mRNAs.[2–4] The functions of ADARs in known substrates suggest that the enzymes function to fine-tune and optimize many biological pathways. Thus, RNA editing alters codon specificity and therefore the amino acid sequence of the encoded protein, resulting in multiple protein products with differing biological functions from a single mRNA precursor. RNA editing represents an important programming mechanism for increasing genetic diversity in eukaryotes. In all cases, pre-mRNA editing requires a double-stranded RNA (dsRNA) structure that is formed between exonic sequences encompassing the editing site and downstream intronic sequences. The genomes of *Saccharomyces cerevisiae* and prokaryotes do not encode classical ADAR proteins. On the basis of sequence homology to ADARs, a yeast protein has been identified that contains a deaminase domain, but lacks a known RNA-binding motif.[5] The deaminase catalyzes deamination of adenosine at position 37 in yeast $tRNA^{ala}$ and was, therefore, named adenosine *dea*minase acting on *t*RNA 1 and its gene tRNA-specific adenosine deaminase 1 (scADAT1/TAD1).[5] ADAT1 proteins have also been cloned from the human,[6] mouse,[3] and *D. melanogaster*,[7] and the first prokaryotic tRNA editing enzyme from a bacterium (*E. coli*, TadA) identified.[8] Recently, the crystal structures of TadA proteins from three different bacterial species, and in complex form with RNA, have been determined.[9–11] By this report, we describe the crystal structure of a tRNA-specific adenosine deaminase (TAD) from *Streptococcus pyogenes*, which was determined at 2.0 Å resolution by multiwavelength anomalous dispersion (MAD) using bound zinc ion. The structure reveals an enzyme that form a homodimer with each monomer consisting of typical α/β fold domains and a long α-helical of C-terminus, a

Coordinates have been deposited in the Protein Data Bank (accession code 2NX8).
Grant sponsor: MOST, Korea; Grant number: M10420010001-04N2001-00110; Grant sponsor: 21 C Functional Proteomics Center, Korea Ministry of Science and Technology and KU research funds.
Won-Ho Lee and Young Kwan Kim contributed equally to this work.
**Correspondence to:* Kwang Yeon Hwang, Division of Biotechnology, College of Life Sciences and Biotechnology, Korea University, Seoul 136-701, South Korea.
E-mail: chahong@korea.ac.kr
Received 24 November 2006; Revised 9 January 2007; Accepted 22 January 2007
Published online 6 June 2007 in Wiley InterScience (www.interscience.wiley.com).
DOI: 10.1002/prot.21456

Table I
Statistics From the Crystallographic Analysis

Data set		Zn-MAD	
Space group		$P4_22_12$	
Resolution (Å)	2.0	2.0	2.0
	peak	*edge*	*remote*
Wavelength	1.2834	1.2827	1.2573
Unique reflections	17,584	16,689	16,365
Data coverage (%)	93.6	88.4	86.2
R_{sym}[a] (%)	8.0	7.0	7.5
Mean FOM[b] (20.0–2.8 Å)	0.60		
Refinement statistics	(50.0–2.0 Å) Apo		
Rmsd[c]			
Bonds (Å)	0.006		
Angles (degree)	1.00		
Reflections ($\|F\| > 1\sigma$)	27,909		
Total atoms	1,324		
R-factor[d] (%)	21.4		
R_{free}[e] (%)	24.2		

[a] $R_{sym} = \Sigma_h\Sigma_i|I_{h,i} - \langle I_{h,i}\rangle|/\Sigma_h\Sigma_i\Sigma_{h,i}$ for the intensity (I) of i observations of reflection h.
[b] FOM, Figure of merit.
[c] Root-mean-square deviations from ideal geometry.
[d] *R*-factor $= \Sigma|F_{obs} - F_{calc}|/\Sigma|F_{obs}|$, where F_{obs} and F_{calc} are the observed and calculated structure factors, respectively.
[e] R_{free} = *R*-factor calculated using 10% of the reflections data chosen randomly and omitted from the start of refinement.

unique structure that has been observed in other Tad families. The zinc ion is tetrahedral coordinated by highly conserved residues, one His, two Cysteines, and one water molecule. Our structural results provide insight into the function of conserved residues within the TAD superfamily.

MATERIALS AND METHODS

The cloning, purification, and crystallization of TadA from *Streptococcus pyogenes* has been reported.[12] Briefly, His-tagged TadA in pET22b vector was expressed in an *Escherichia coli* strain BL21 (DE3). The Zn-MAD data sets were collected using a synchrotron radiation source at beamline 4A of Pohang Light Source (PLS, South Korea). MAD data were collected at three wavelengths (peak = 1.2834, edge = 1.2827, remote = 1.2573). The crystals belonged to the space group $P4_22_12$ with $a = b = 80.091$ Å, $c = 81.104$ Å. Data were processed within the program HKL2000 and SCALEPACK.[13]

The structure of TadA from *S. pyogenes* was determined by the multiwavelength anomalous diffraction method using zinc ion of crystal. The phases were calculated with the SOLVE and RESOLVE[14] programs with a mean figure of merit of 0.60 at 2.8 Å resolution. The MAD phasing statistics and refinement statistics are presented in Table I. The model was completed by iterative cycles of model building with Coot[15] and refinement with CNS[16] yielding a final model containing 173 amino acids, one Zn(II) ion, one phosphate ion, and 147 water molecules for TadA. The

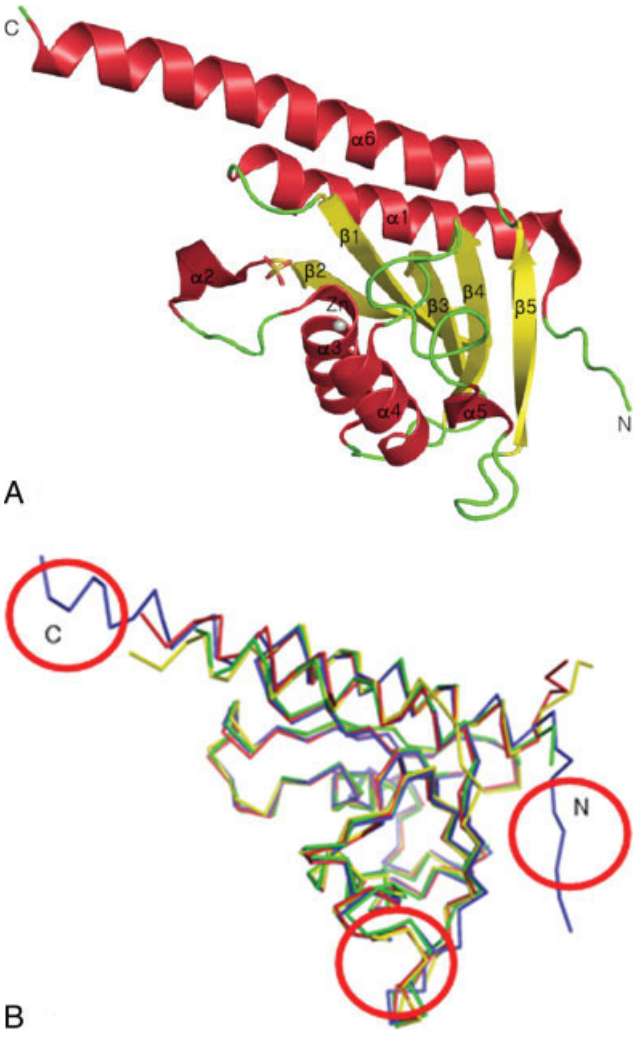

Figure 1
*(**A**) Overall structure A schematic ribbon diagram of the overall structure of the tRNA-specific adenosine deaminase (residues 5-173) from* S. pyogenes *(spTad A). The N- and C-termini of the protein are labeled, and the helices and sheets are numbered. Zn (II) and the phosphate ion are shown in gray sphere and ball-and-stick models, respectively. (**B**) Superimposition of spTadA and other proteins. The overall structure of spTad A is superimposed on other TadA proteins in a ribbon model representation. The blue, yellow, red and green colors are shown to* S. pyogenes *TadA, A. aeolicus TadA (1WWR), E. coli TadA (1Z3A), and* Staphylococcus aureus *TadA (2B3J), respectively. The red circles are shown in the main differences. (**C**) Comparison of active sites between spTadA and saTadA-complexed with RNA. A detailed depiction of the interacting residues of the active site compared to* Staphylococcus aureus *Tad A (saTadA) is shown by ball-and-stick models. In saTadA, the His residue has the π–π interaction with PURINE RIBOSIDE-5′-MONOPHOSPHATE (C_{10} H_{13} N_4 O_7 P) (PR5). Green residues are spTadA, yellow residues the saTad A (2B3J), blue the phosphate ion, PO_4^- (spTad), and red is PR5 (2B3J). (**D**) The dimer interface of spTadA. The monomers interact with each other symmetrically. The residues participated in forming the interfaces are shown as ball-and-stick models and the interaction with another monomer. The hydrogen bonding and hydrophobic interactions are major forces in forming the dimer interface.*

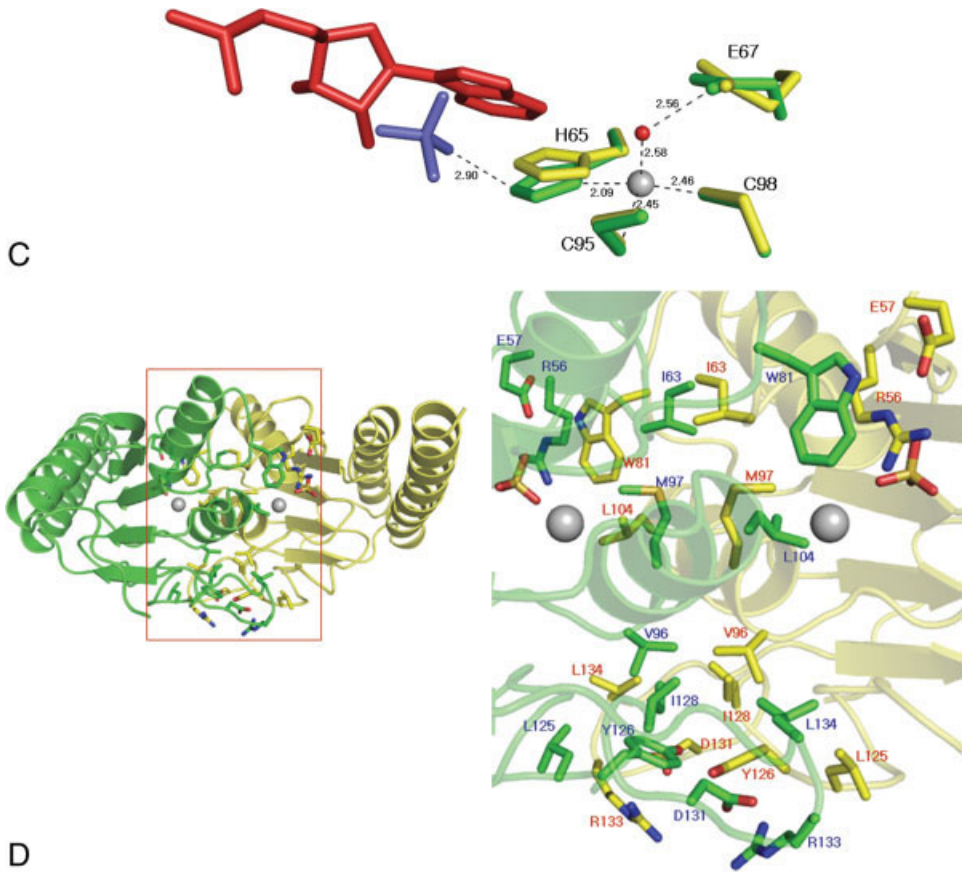

Figure 1
(Continued)

metal content of the crystal was assessed by X-ray fluorescence experiments carried out at Pohang Light Source Beamline 4A near the κ edge for zinc (1.38 Å). We carried out the structure analyses using the following computer programs: Swiss-Pdb-Viewer and Coot for superposition of molecules and secondary structure-based alignment; SSAP server[17] for calculation of the root-mean-square deviations (RMSDs); ES-Pript[18] for preparation of the secondary structure alignment figure; Pymol[19] for the depiction of structure; and GRASP[20] for the calculation and depiction of electrostatic potentials at the molecular surface. Other orthologs used in the structural comparison were *Staphylococcus aureus* (PDB code 2B3J),[9] *E. coli* (PDB code 1Z3A),[10] *A. aeolicus* (PDB code 1WWR).[11]

RESULTS AND DISCUSSION

The structure of TadA from *Streptococcus pyogenes* (*sp*TadA) was determined to a resolution of 2.0 Å using the multiwavelength anomalous dispersion (MAD) method with zinc ion. The crystal shows symmetry of the space group $P4_22_12$ and contains one molecule in the asymmetric unit. The monomer is a classical α/β/α protein of approximate dimensions 31 × 33 × 58 $Å^3$ [Fig. 1(a)]. The structure consists of a central β-sheet with two α-helices (α1, α6) on one side of the sheet and three α-helices (α3–α5) on the other side. The overall folding of *sp*TadA is similar to that of other bacteria, TadA from *Staphylococcus aureus* (PDB code 2B3J),[9] *Escherichia coli* (PDB code 1Z3A),[10] *Aquilfex aeolicus* (PDB code 1WWR),[11] with an overall Cα rms deviations of 0.75, 0.75, and 1.45 Å, respectively. The main differences are found in the loop and 3_{10}-helix (α5) between β4 and β5, the additional region of the N-terminal and the long C-terminal α-helix. A superposed illustration is shown in Figure 1(b). Additional structural analyses show that *sp*TadA have high similarity in the shape of the active site cavities and distribution of conserved residues on and around the surface of the cavities. Although the residues that comprised the cavities are mostly conserved, there are still some nonconserved residues distributed on the surface of the cavities. The notable C-terminal long helices functioning to cap the active site of the cavity in *sp*TadA structures may play

DOI 10.1002/prot

role in binding specific tRNA substrates. The simulated annealing omit map showed a marked electron density peak located within 2.0–2.5 Å from His65, Cys95, and Cys98. The Zn^{2+} absorption edge was determined to be 1.38 Å in an X-ray absorption experiment. The position of the bound Zn^{2+} in *sp*TadA is very similar to that in the other TadA structures (rms deviation 0.2 Å). The Zn^{2+} ion located at the bottom of the active site is coordinated by the Nδ1 atom of His65 (2.1 Å), Sγ atom of Cys95 (2.4 Å), Sγ atom of Cys98 (2.4 Å), and a water molecule (2.46 Å) with a slightly distorted tetragonal geometry. Interestingly, we found a phosphate ion near the active site that is formed by the hydrogen bonding with Nε2 of His65 (2.7 Å). When our structure was superimposed with the complex-tad structure (pdb1WWR), this position coincided with the RNA substrate [Fig. 1(c)].

The purified *sp*TadA ran at an apparent molecular weight of 38 kDa on a gel-filtration column, approximately twice the expected molecular weight of 19 kDa. The dimer appears to be the physiological condition with the crystallographic packing showing that the *sp*TadA forms a dimer when in a solution. The dimer interface is formed around the helix α4 with a crystallographic two-fold symmetry through hydrogen bonding, salt bridging, and hydrophobic interactions [Fig. 1(d)]. Dimer formation decreases the accessible surface by 1,684.3 $Å^2$ per monomer or 15.4% of the total surface of the monomer. Among the buried surface residues, 48.4% are hydrophobic, 19.4% are polar, and 29.0% are charged indicating that the majority of the dimeric interface is formed by hydrophobic and nonpolar interactions. From the structural aspects, dimerization appears to be important for specific binding with tRNA and enzyme functions. Firstly, the shape and charge distribution of the dimer surface is suitable to bind with tRNA and secondly, most of the dimer interface is nonpolar. The formation of a dimer, therefore, would be energetically favorable compared with the monomer in solution.

In summary, we have determined the three-dimensional structure of the *sp*TadA at 2.0 Å. The arrangements of the active site residues and the interactions among them have been elucidated and provide a clearer understanding of the mechanism for catalysis by the enzyme. Structure comparisons reveal some different structural characteristics between *sp*TadA and other TadAs species.

ACKNOWLEDGMENTS

We thank Dr. H. S. Lee and his staff for assistance during data collection at beamline 4A of Pohang Light Source, Korea.

REFERENCES

1. Holley RW. Structure of an alanine transfer ribonucleic acid. J Am Med Assoc 1965;194:868–871.
2. Bass BL. RNA editing and hypermutation by adenosine deamination. Trends Biochem Sci 1997;22:157–162.
3. Maas S, Kim YG, Rich A. Sequence, genomic organization and functional expression of the murine tRNA-specific adenosine deaminase ADAT1. Gene 2003;243:59–66.
4. Gerber A, Keller W. RNA editing by base deamination: more enzymes, more targets, new mysteries. Trends Biochem Sci 2001;26: 376–384.
5. Gerber A, Grosjean H, Melcher T, Keller W. Tad1p, a yeast tRNA-specific adenosine deaminase, is related to the mammalian pre-mRNA editing enzymes ADAR1 and ADAR2. EMBO J 1998:17; 4780–4789.
6. Maas S, Gerber AP, Rich A. Identification and characterization of a human tRNA-specific adenosine deaminase related to the ADAR family of pre-mRNA editing enzymes. Proc Natl Acad Sci USA 1999;96:8895–8900.
7. Keegan LP, Gerber AP, Brindle J, Leemans R, Gallo A, Keller W, O'Connell MA. The properties of a tRNA-specific adenosine deaminase from *Drosophila melanogaster* support an evolutionary link between pre-mRNA editing and tRNA modification. Mol Cell Biol 2000;20:825–833.
8. Wolf J, Gerber AP, Keller W. TadA, an essential tRNA-specific adenosine deaminase from *Escherichia coli*. EMBO J 2002;2:3841–3851.
9. Losey HC, Ruthenburg AJ, Verdine GL. Crystal structure of *Staphylococcus aureus* tRNA adenosine deaminase TadA in complex with RNA. Nat Struct Mol Biol 2006;13:153–159.
10. Kim J, Malashkevich V, Roday S, Lisbin M, Schramm VL, Almo SC. Structural and kinetic characterization of *Escherichia coli* TadA, the wobble-specific tRNA deaminase. Biochemistry 2006;23;45(20):6407–6416.
11. Kuratani M, Ishii R, Bessho Y, Fukunaga R, Sengoku T, Shirouzu M, Sekine S, Yokoyama S. Crystal structure of tRNA adenosine deaminase (TadA) from *Aquifex aeolicus*. J Biol Chem 2005;280:16002–16008.
12. Ku MJ, Lee W-H, Hwang KY. Crystallization and preliminary X-ray crystallographic analysis of the tRNA-specific adenosine deaminase from *Streptococcus pyogenes*. Acta Cryst F 2005;375–377.
13. Otwinowski Z, Minor W. Processing of X-ray diffraction data collected in oscillation mode. Methods Enzymol 1997;276:307–326.
14. Terwilliger TC. SOLVE and RESOLVE: automated structure solution and density modification. Methods Enzymol 2003;374:22–37.
15. Paul E, Kevin C. Coot: model-building tools for molecular graphics. Acta Crystallogr D 2004;60:2126–2132.
16. Brünger AT, Adams PD, Clore GM, Delano WL, Gros P, Grosse-Kunstleve RW, Jiang J-S, Kuszewski J, Nilges N, Pannu NS, Read RJ, Rice LM, Simonson T, Warren GL. Crystallography & NMR System: a new software suite for macromolecular structure determination. Acta Crystallogr D 1998;54:905–921.
17. Orengo CA, Michie AD, Jones S, Jones DT, Swindells MB, Thornton JM. CATH—a hierarchic classification of protein domain structures. Structure 1997;5:1093–1108.
18. Gouet P, Courcelle E, Stuart DI, Metoz F. ESPript: analysis of multiple sequence alignments in PostScript. Bioinformatics 1999;14:305–308.
19. DeLano WL. The PYMOL Molecular Graphics System. San Carlos, CA: DeLano Scientic LLC; 2002. http://pymol.sourceforge.net.
20. Nicholls A, Sharp KA, Honig B. Protein folding and association: insight from the interfacial and thermodynamic properties of hydrocarbons. Proteins 1991;11:281–296.